

# RESPONSE PREDICTION AND DAMAGE EVALUATION OF A REINFORCED CONCRETE STRUCTURE BASED ON LIMITED SENSOR DATA AND THE KALMAN METHOD

Zhuoran YI<sup>1</sup>, Ayumi OONO<sup>2</sup>, Jonathan MONICAL<sup>3</sup>, Masaki MAEDA<sup>4</sup>

## ABSTRACT

The response and damage level of a reinforced concrete structure is evaluated using a simulated performance curve updated by the Kalman method to match the observed response of a 1/4-scale four-story reinforced concrete frame with shear walls subjected to a series of earthquake simulation tests. The capacity spectrum method is used to estimate structural response with the damping model updated by Kalman method. Damage levels are defined using characteristic points. Estimated drift error is within 35% of measured drift, and the predicted damage level matches well with the observed damage level.

**Keywords:** Reinforced concrete, Response prediction, Damage evaluation, Kalman method

## 1. BACKGROUND

Reinforced concrete structures should be evaluated for damage quickly after intense earthquakes [1]. By surveying damaged structures, engineers can judge the current condition of the structure and predict damage in future ground motions. However, quantifying damage through visual inspection requires time and skilled labor. A structural health monitoring (SHM) system is a viable alternative solution because it can record drift and acceleration demands of the structure and output measurements automatically. Hence, it is possible to evaluate the damage level of the structure using the data provided by the SHM system [2-3].

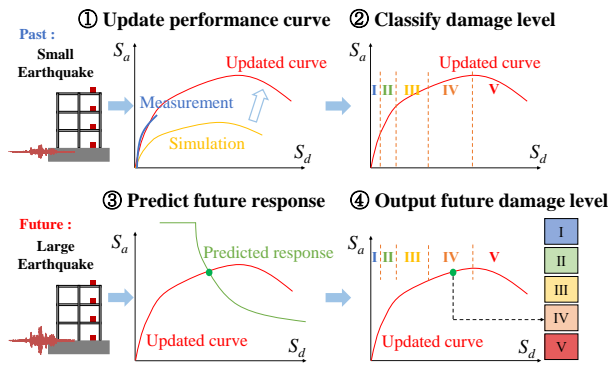


Fig.1 Description of research target

The purpose of this paper is to evaluate the future damage level of a structure, not yet observed in past earthquakes, using the data provided by the SHM system. A Kalman filtering method is applied to update the performance curve and damping model. As shown in Fig.1, the main goals are to develop methods to (1) update the simulated performance curve to match the

observed response, (2) propose and evaluate damping behavior in the linear and nonlinear range of response relative to measured damping behavior, and (3) predict response and damage levels of a reinforced concrete building in future earthquakes using measured data obtained from sensors in past earthquakes. The proposed method is expected to be applied to evaluate the residual seismic performance of RC buildings quickly.

## 2. INTRODUCTION OF KALMAN METHOD

The Kalman filtering method produces an updated model by considering errors associated with measurement and simulation [3-4]. The fundamental concept is illustrated in Figs. 2-3. Each step of the Kalman method is described next.

- ① Use the value and error at  $x_i$  to predict the value and error at the next step  $x_{i+1}$  using the theoretical model (Eq. 1)

$$y_{i+1} = a_i(x_{i+1} - x_i) + y_k + R \quad (1)$$

where  $y_k$  is the updated value at  $x_i$ ,  $y_{i+1}$  is the value predicted by the theoretical model  $y=a_ix+b$ , and  $R$  is a constant error associated with measurement. The errors  $Py$  and  $Pa$  corresponding to values  $y$  and  $a$  are shown as a covariance matrix and updated based on Eq. (2).

$$P_{i+1} = \begin{bmatrix} Py_{i+1} \\ Pa_{i+1} \end{bmatrix} = \begin{bmatrix} 1 & x_i - x_{i-1} \\ 0 & 1 \end{bmatrix} \cdot \begin{bmatrix} Py_{ki} \\ Pa_{ki} \end{bmatrix} \cdot \begin{bmatrix} 1 & x_i - x_{i-1} \\ 0 & 1 \end{bmatrix}^T \quad (2)$$

where  $Py_{ti}$  and  $Pa_{ti}$  are the updated errors predicted by the theoretical model at  $x_i$ , and  $P_{i+1}$  is the error predicted by the theoretical model  $y=a_{i+1}x+b$ .

- ② Calculate Kalman gain  $K_{i+1}$  using the predicted error  $P_{i+1}$  and measurement error  $R$  with Eq. (3).

$$K_{i+1} = P_{i+1} / (P_{i+1} + R) \quad (3)$$

- ③ Use Kalman gain  $K_{i+1}$  to update the data  $y_{i+1}$ ,  $a_i$ , and error  $P_{i+1}$  to  $y_{ki+1}$ ,  $a_{i+1}$ , and  $P_{ki+1}$  with Eqs. (4)-(5)

\*1 Ph.D Student, Graduate School of Engineering, Tohoku University, JCI Student Member

\*2 Undergraduate Student, School of Engineering, Tohoku University, JCI student Member

\*3 JSPS Researcher, Dept. of Architecture and Building Science, Tohoku University, Dr. Eng., JCI Member

\*4 Professor, Dept. of Architecture and Building Science, Tohoku University, Dr. Eng., JCI Member

$$\begin{bmatrix} y_{ki+1} \\ a_{i+1} \end{bmatrix} = \begin{bmatrix} y_{ii+1} \\ a_i \end{bmatrix} + K_{i+1}(y_{m+1} - y_{ii+1}) \quad (4)$$

where  $y_{m+1}$  is the measured value at  $x_{i+1}$ .

$$P_{ki+1} = P_{ii+1} - K_{i+1}P_{ii+1} \quad (5)$$

- ④ The updated values  $y_{ki+1}$ ,  $a_{i+1}$ , and  $P_{ki+1}$  become the initial parameters for the updating process in the next step.

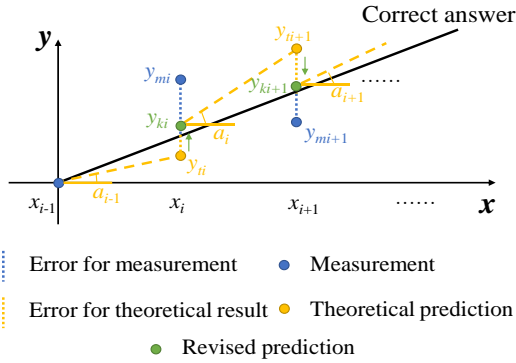


Fig.2 Basic principle of Kalman method

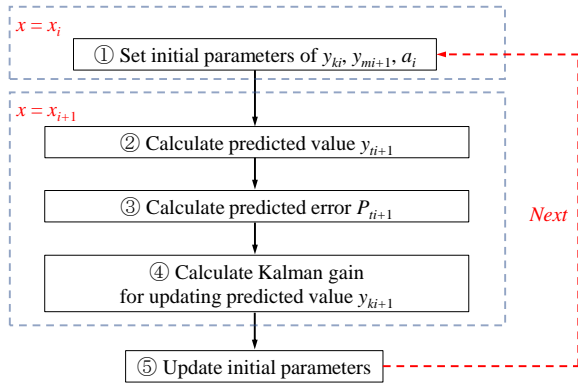


Fig.3 Flow chart for Kalman method

Using the five steps described above, the Kalman method produces an updated prediction  $y_k$  for each consecutive time step where the errors relative to the simulated model and observed response are expected to decrease with time.

### 3. EXPERIMENTAL DATA AND SIMULATION

#### 3.1 Kalman method applied to experimental data

In this paper, the Kalman method is applied to the results of a shaking table test of a 1/4-scale four-story reinforced concrete frame with shear walls [5] shown in Fig. 4. Nine earthquake simulations listed in Tab. 1 were used as the input ground motions.

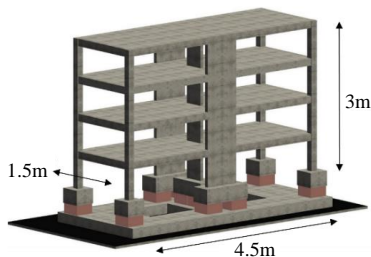


Fig.4 3D view of the test specimen

Table 1. Input ground motions

Run	Acceleration spectrum	Phase	Amplification factor $\alpha$ (%)		Damage level (x)
			x	y	
1			20	20	I
2			80	60	I
3	5%-damped	JMA Kobe	160	100	I
4	acceleration		240	150	III
5	response		260	170	IV
6	spectra of the		130	100	/
7	AIJ standard		220	120	/
8			220	/	/
9			260	/	IV

Both the simulation and experiment have the same total collapse mechanism. The four-story structure is reduced to a single-degree-of-freedom (SDOF) system. The maximum Spectral acceleration ( $S_a$ ) and Spectral displacement ( $S_d$ ) reached in each run is used to generate the measured performance curve. A static push-over analysis of the specimen was conducted with a frame analysis program called SNAP and the simulated performance curve of an equivalent SDOF system was obtained. Measured and simulated performance curves are plotted in Fig. 5. Because the intensities of simulated motions used in Runs 6-8 are smaller than the intensity of the motion used in Run 5, Runs 6-8 are ignored in the following sections.

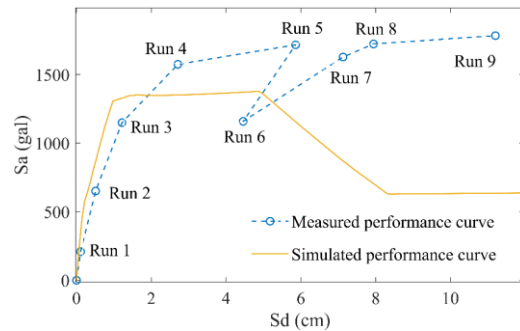


Fig.5 Performance curves

#### 3.2. Calculation of measured damping factor

The Japanese seismic design code offers a reduction factor  $F_h$  for a response spectrum  $S$  used in the Capacity Spectrum Method (CSM) calculated with Eq. (6)

$$F_h = 1.5/(1 + 10h) \quad (6)$$

where  $h$  is the equivalent damping factor. As shown in Fig. 6, the standard response spectrum  $S_0$  is multiplied by an amplification factor  $\alpha$  based on the amplitude of the input motion.  $S_0$  is the standard spectrum based on soil condition according to the Japanese building design code.

Measured damping factors are evaluated using the Capacity Spectrum Method as illustrated in Fig. 6. The method estimates seismic demand as the intersection of the response spectrum and performance curve. To estimate a plausible reduction factor  $F_h$  and thus damping factor  $h$  associated with the observed response, damping is incrementally increased to reduce the response spectrum in an iterative fashion until the

intersection of the curves produces a solution equivalent to the measured response. The equivalent damping factor  $h$  may be evaluated based on measured response  $S_m$  with Eq. (7) and (8).

$$S_m = F_h \cdot \alpha \cdot S_0 = \alpha \cdot S_0 \cdot 1.5 / (1 + 10h) \quad (7)$$

$$h = 0.1 \times (1.5\alpha \cdot S_0 / S_m - 1) \quad (8)$$

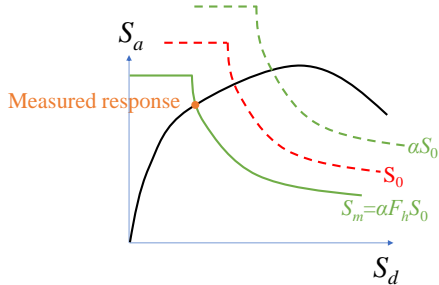


Fig.6 Capacity Spectrum Method used to obtain measured damping

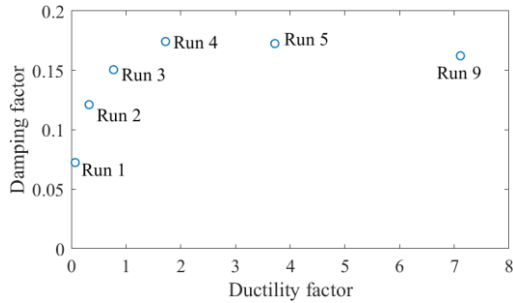


Fig.7 Estimates of measured damping

#### 4. UPDATED PERFORMANCE CURVE

In this section, the performance curve is updated based on simulated and measured performance curves for a limited number of runs. The updating method is explained next.

##### 4.1 Introduction of method

Because the measured performance curve is expressed as several line segments connecting points of the peak response reached in each run, it may be inaccurate. Therefore, the performance curve is smoothed by the Kalman filtering method using the measured performance curve as the input measurement data and the simulated performance curve as the simulated input data as illustrated in Fig. 8.

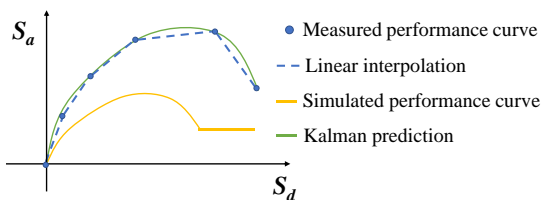


Fig.8 Concept of Smoothing method

After smoothing, the lateral stiffness and rate of change of lateral stiffness is calculated using the slope of the smoothed performance curve as shown in Fig. 9. The tangential stiffness  $K$  of a structure may change rapidly

as damage such as cracking and yielding occurs. Hence, the local maximum points of the rate of change of stiffness are identified as “characteristic points” of the observed response of the structure. The characteristic points of the simulated model may also be identified from the simulated performance curve using the same procedure.

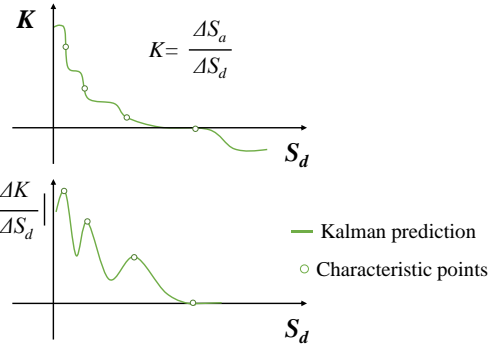


Fig.9 Identification of characteristic points

After the characteristic points are identified, the simulated performance curve is updated so that the characteristic points of both of measured and simulated curves will match as shown in Fig. 10. The simulated performance curve is updated by fitting each simulated characteristic point with the corresponding measured characteristic point using a series of amplification factors  $\alpha_i$  and  $\beta_i$  for  $S_a$  and  $S_d$ .

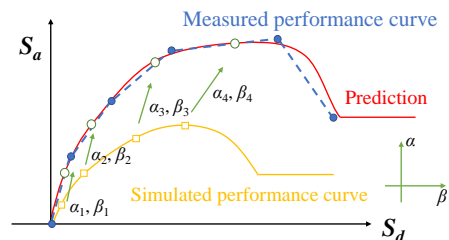


Fig.10 Concept of Updating  $S_a$ - $S_d$  curve

##### 4.2 Updated results

The method described in Sec. 4.1 is applied to the mentioned shake table experiment. Fig. 11 shows the performance curves and Tab. 2 lists the identified characteristic points.

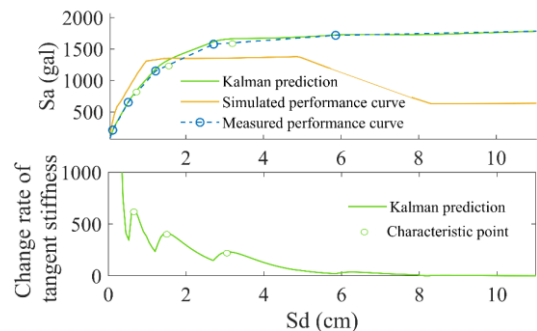


Fig.11 Identified characteristic points

Considering cases where data is available until Run 3, 4, 5, and 9, the updated performance curves are plotted in Fig. 12. All of the updated performance curves

are similar to the measured performance curves, indicating the reliability of the proposed method.

Characteristic points		$S_a$ (gal)	$S_d$ (cm)
Measured performance curve	Cracking	799	0.68
	First yielding	1309	1.50
	Flexural mechanism	1660	3.15
Simulated performance curve	Cracking	581	0.23
	First yielding	1310	1.98
	Flexural mechanism	1349	1.58

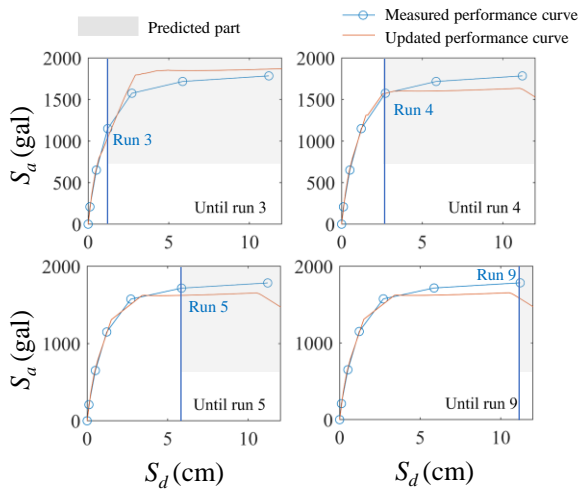


Fig.12 Updated results using limited data

### 5. DAMAGE LEVEL CLASSIFICATION

The characteristic points identified in Sec. 4 are used to describe the damage behavior of the structure. Characteristic points including initial cracking, initial yielding, flexural mechanism, and ultimate state are assumed to represent reasonable boundaries between distinct levels of damage. The relationship between the selected characteristic points and damage levels is shown in Tab. 3. The boundary  $S_d$  between damage levels III and IV is defined as the midpoint between  $S_d$  at flexural mechanism and  $S_d$  at ultimate state points.

Level	Description	Characteristic points
0	No damage	Before initial cracking
I	Slight	After initial cracking
II	Minor	After initial yielding
III	Moderate	After flexural mechanism
IV	Severe	Before ultimate point
V	Collapse	After ultimate point

Damage levels evaluated using the procedure described in Tab. 3 are plotted in Fig. 13 and compared with measured results in Fig. 14. Measured damage levels are obtained using the residual seismic capacity ratio index  $R$  defined by the Japanese Damage Evaluation Standard [6] based on the observed response. The predicted damage level evaluated with the method

proposed here, although slightly overestimated, matches well with the measured damage level.

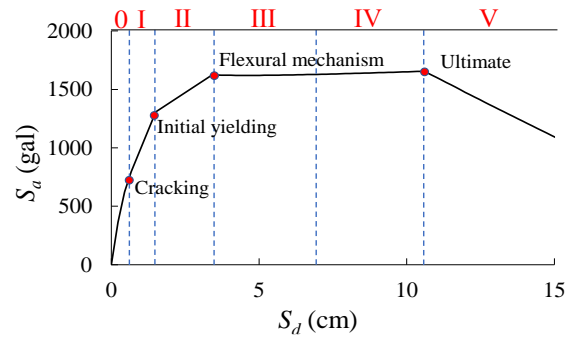


Fig.13 Damage classification using data until Run4

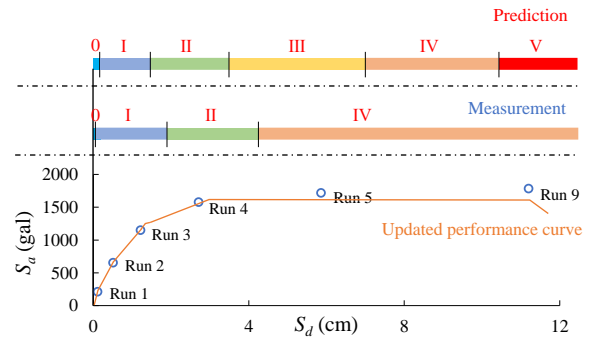


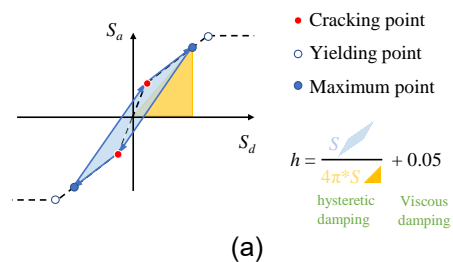
Fig.14 Measured and predicted damage levels

### 6. PREDICTION OF FUTURE RESPONSE

This section describes the accuracy of predicting future response evaluated using 1) the Capacity Spectrum Method and 2) measured data obtained in runs associated with different levels of damage. Based on previous studies [2-3,7], the prediction of nonlinear response based on runs in the linear range of response produces large errors. To increase the accuracy of the prediction, the theoretical damping model must incorporate the influence of hysteretic damping on structural response before yielding.

#### 6.1 Calculating damping using the Takeda model

The Takeda model defines cracking and yielding in load-displacement relationships for reinforced concrete structures and is studied here to describe the relationship between ductility factor and theoretical damping before and after yielding (Fig. 15). Theoretical damping is computed as the ratio of energy dissipation (blue area) to maximum elastic potential energy (yellow area). Cracking and yielding points identified in Sec. 4 are utilized in the calculation.



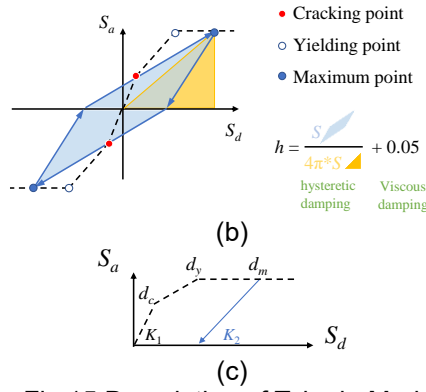
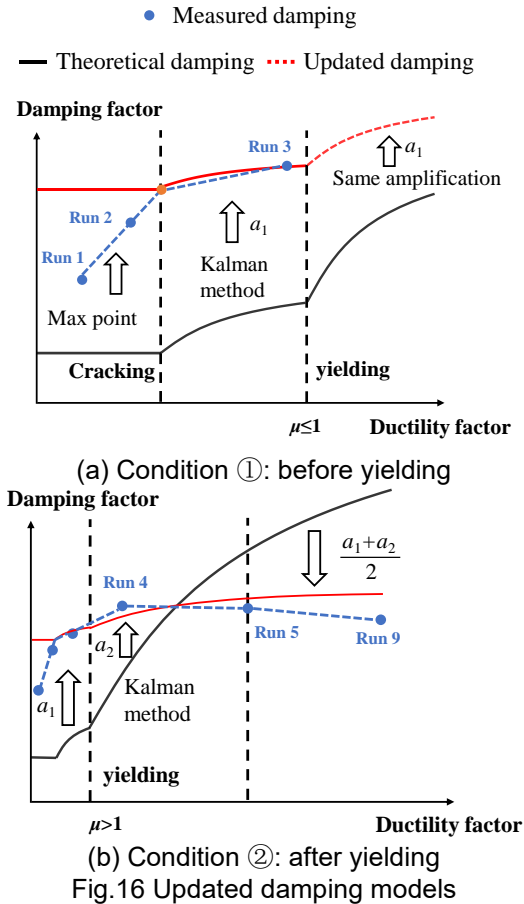


Fig.15 Description of Takeda Model  
 (a) Damping calculation before yielding  
 (b) Damping calculation after yielding  
 (c) Unloading stiffness

### 6.2 Updated prediction of damping

To produce more accurate estimates of damping before and after yielding, the theoretical damping model is updated using Kalman and amplification methods considering the two conditions illustrated in Fig. 16.



Condition ①: Using data before yielding (Runs 1-3)

Condition ① predicts damping in Runs 4-9. The predicted yielding point is used instead of the measured yielding point because it is unknown until Run 4. Before cracking, the updated damping factor is constant and is equal to the maximum measured damping factor. After cracking and before initial yielding, the Kalman method

is used to update theoretical damping using an amplification factor calculated using the known measured data. Damping is predicted in the nonlinear range of response by updating the theoretical damping model using the same amplification factor calculated in the linear range of response.

Condition ②: Using data after yielding (Runs 4-5)

The measured cracking point and initial yielding point are used to update the theoretical damping model in Condition ②. Before yielding, the updating method is the same as Condition ①. After yielding, a separate amplification factor is computed considering measured data in the nonlinear range of response only. The average of the two amplification factors (computed before and after yielding) is used with the Kalman method to update the theoretical damping model in the nonlinear range of response. The updated damping factors for each condition are shown in Fig. 17.

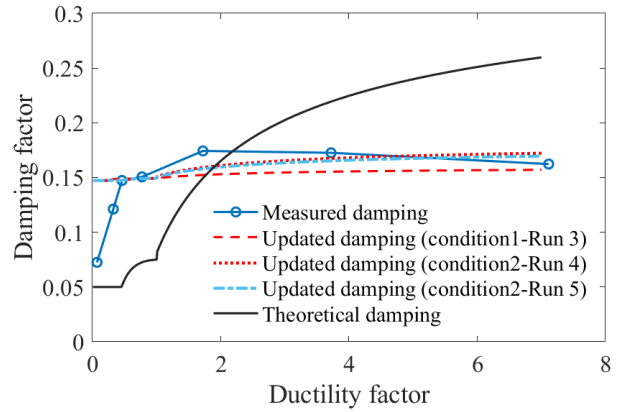


Fig.17 Updated damping using limited data

### 6.3 Response prediction using updated damping

Using the updated damping model described in Sec. 6.2, the future response is estimated using CSM and plotted in Fig.18.

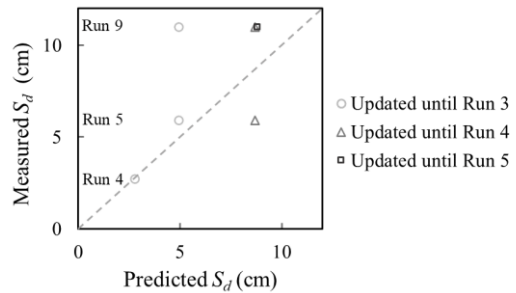


Fig.18 Response prediction

An error  $e_d$  defined by Eq. (9) is utilized to evaluate the accuracy of the prediction method.  $d_{pi}$  and  $d_{mi}$  are the predicted and measured spectral displacements for Run  $i$ . Assuming measured data is known up to Run  $k$ , the error is computed considering Run  $k+1$  to Run 9 (where no measured data is known) and is tabulated in Tab.4.

$$e_d = \sum_{i=k+1}^9 |(d_{pi} - d_{mi}) / d_{mi}| \quad (9)$$

Table 4. Predicted response  $S_d$  (cm)

Run	Measured response	Until Run 3	Until Run 4	Until Run 5
Run 4	2.7	2.8	/	/
Run 5	5.9	5.0	8.7	/
Run 9	11	5.0	8.7	8.8
$e_d$ (%)	/	24	34	20

The structure remained linear in Run 3 and hence no measured yielding point was known yet, the predicted displacements matched well with the measured data in the nonlinear range of response, producing an average error of 24% considering the prediction of Run 4 to 9.

## 7. PREDICTION OF DAMAGE LEVEL

The classification of damage in Sec. 5 and the Capacity Spectrum Method described in Sec. 6 are used to predict damage caused by future earthquakes. The predicted damage level is evaluated assuming measured data is known up to Runs 3, 4, and 5 as shown in Fig. 19. The damage level tends to be underestimated if the structure remains linear (Run 3). However, if the structure yields, the predicted and measured damage levels are the same. Besides, since the proposed method is only verified by one experiment, more cases are needed to verify the workability in the future.

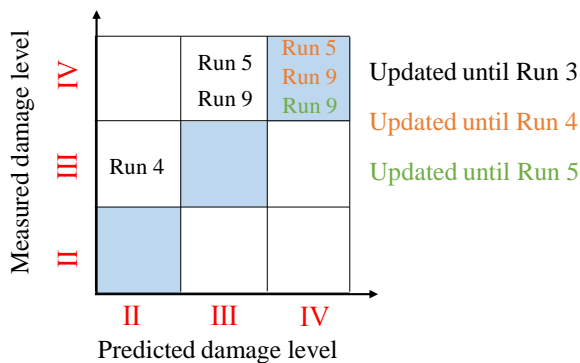


Fig.19 Damage level prediction

## 8. CONCLUSIONS

The following three conclusions are drawn:

- A procedure for updating the simulated performance curve of a 4-story RC structure using the Kalman method, characteristic points, and limited measured data produces a predicted response similar to the response observed in earthquake simulation tests.
- The future response evaluated using the Capacity Spectrum Method, an updated damping model, and measured data in the linear range of response only

produced reliable estimates of nonlinear displacement demands with an average error of approximately 25%.

- Damage levels evaluated using measured data in the nonlinear range of response agree with observed damage levels. In runs when the structure remained linear, damage tends to be underestimated by one level.

## ACKNOWLEDGEMENT

This work was supported by JAEA Nuclear Energy S&T and Human Resource Development Project “建屋応答モニタリングと損傷イメージング技術を活用したハイブリッド型の原子炉建屋長期健全性評価法の開発研究” (Grant Number JPJA21P12345678, Principal researcher: Prof. Masaki MAEDA, Tohoku University). This work would like to thank Dr. Benjamin and Dr. Seki for the excellent comments.

## REFERENCES

- [1] Datta, T., “Seismic analysis of structures”. John Wiley & Sons, Ltd. 2010, pp. 369.
- [2] Yi, Z., Oono, A., et al., “加速度センサによる観測記録に基づく鉄筋コンクリート建物の応答予測と被害推定 その2 Response prediction and damage evaluation of a reinforced concrete structure”, Paper No. TS 20220166, JAEE, 2022.
- [3] Oono, A., Yi, Z., et al., “加速度センサによる観測記録に基づく鉄筋コンクリート建物の応答予測と被害推定 その1 性能曲線の修正方法についての検討”, Paper No. TS 20220148, JAEE, 2022.
- [4] Xu, K., and Mita, A., “Estimation of maximum drift of multi-degree-of-freedom shear structures with unknown parameters using only one accelerometer,” Structural Control and Health Monitoring, May. 2021, pp.1-20 (28:e2799).
- [5] Miura, K., Fujita, K., Tabata, Y., Maeda, M., Shegay, A. & Yonezawa, K., “Shake-table test of A 4-Story frame-wall RC structure to investigate the collapse mechanism and safety limit”, Journal of Structural and Construction Engineering., Vol. pp. 247-257, Feb. 2021.
- [6] Japan Building Disaster Prevention Association, “Damage Level Evaluation Standard for Reinforced Concrete Buildings”, 2015.
- [7] Nashimoto, Y., Kikuchi, Y., Suzuki, Y. & Maeda, M., “Quick post-earthquake damage evaluation for rc buildings based on successive modification of analytical model with feedback of observed seismic response”, AIJ Journal of Technology and Design., Vol. 23, pp. 497-500, Jun. 2017.